



A new pH-sensitive fluorescent probe for visualization of endoplasmic reticulum acidification during stress



Haibin Xiao¹, Ruilin Zhang¹, Chuanchen Wu, Ping Li*, Wen Zhang*, Bo Tang

College of Chemistry, Chemical Engineering and Materials Science, Collaborative Innovation Center of Functionalized Probes for Chemical Imaging in Universities of Shandong, Key Laboratory of Molecular and Nano Probes, Ministry of Education, Institute of Biomedical Sciences, Shandong Normal University, Jinan 250014, PR China

ARTICLE INFO

Keywords:

Fluorescent probe
Endoplasmic reticulum
pH
In vivo imaging
Stress

ABSTRACT

A novel pH-sensitive fluorescent probe termed ER-H for visualization of ER acidification during ER stress in living cells and in vivo was presented. ER-H consists of a piperazine-linked 1,8-naphthalimide as a fluorescence turn-on signaling unit, a 4-methyl benzenesulphonamide moiety for ER anchoring, and a thiol reactive benzyl chloride subunit for biomacromolecules fixation at the ER. ER-H displays sensitive fluorescence enhancement under acidic condition, thus enabling it to monitor ER acidification. Meanwhile, ER-H shows negligible response to common species, high photostability and low cytotoxicity. In biological experiments, the probe ER-H can solely accumulate into ER and track the acidification during ER stress. By combining ER-H with calcium ion sensor Fluo-3 AM, we achieved the simultaneous fluorescence imaging of decrease of ER pH and increase of cytoplasmic calcium ion. Additionally, the probe was also utilized for fluorescence imaging of the acidification in zebrafish and mice model successfully. We thus believe that ER-H has great potential as a practical tool for real-time monitoring of the acidification of ER, contributing to revealing the pathogenesis of ER stress associated diseases.

1. Introduction

Endoplasmic reticulum (ER) as an essential organelle is central in calcium homeostasis, lipid synthesis and folding as well as maturation of membrane and secretory proteins [1–3]. When normal functions of the ER was disturbed by various conditions, such as glucotoxicity, ER Ca²⁺ disequilibrium, ischemia and hypoxia, free radicals, increased protein synthesis, ER stress will appear [4–6]. Recently, a number of studies have demonstrated the crucial role of ER stress in the development of many metabolic diseases, including obesity, insulin resistance, and diabetes [7,8]. For instance, the markers of ER stress are elevated in diabetic animals and therapeutic strategies that manipulate components of the ER stress response will improve normal function in the setting of diabetes. This indicates that targeting ER stress may be a viable treatment option to prevent or attenuate the development of corresponding diseases.

Intracellular pH plays a vital role in many cellular events, such as cell growth, apoptosis, ion transport, autophagy, enzymatic activities, homeostasis and other cellular processes [9–11]. In particular, the pH of ER as a vital parameter is important for regulating the normal physiological function of this organelle [12]. Numerous studies showed that ER stress can trigger autophagy, leading to the acidification of ER

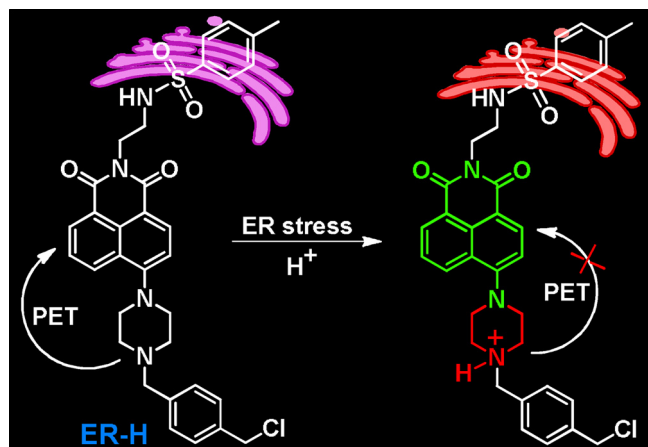
[13–15]. As a perturbation of homeostasis, the ER acidification process is closely related to the progress of ER stress induced diseases [16]. Therefore, owing to the physiological significance of ER pH and acidification, it's of great importance to real-time visualize the pH changes inside ER during stress for elucidating cellular metabolisms and gaining insights into pathogenesis of associated diseases.

Fluorescence imaging is emerging as a promising and powerful means for monitoring various bioactive molecules in living systems, which thanks to its remarkable advantages, such as easy operation, high sensitivity and high temporal-spatial resolution [17,18]. Specifically, two-photon fluorescence microscopy imaging is a fascinating approach utilizing near-infrared laser pulses, which exhibits lots of merits including deeper tissue penetration, higher spatial resolution with minimum background emission, and longer observation time. Therefore, many fluorescent probes with one- or two-photon property for various bioactive molecules have been reported in recent years, which has facilitated progress in cell biology and therapeutics imaging [19–27]. Among them, many pH-responsive sensors have been presented, which has uncovered the chemical biology of pH to some extent [28–42]. However, up to now, fluorescent probe suitable for imaging of pH in ER, especially visualizing the ER acidification in real-time hasn't been presented.

* Corresponding authors.

E-mail addresses: zhangwen@sdnu.edu.cn (P. Li), lip@sdnu.edu.cn (W. Zhang).

¹ These authors contribute equally to this work.



Scheme 1. The structure of ER-H and proposed sensing mechanism for pH.

To solve this issue, new pH-sensitive fluorescent probe should be explored. Motivated to meet this need, specific conditions must be considered: 1) the probe should have a turn-on fluorescence response to acidic pH value; 2) the probe must possess outstanding ER-targetable ability; 3) the probe should have two-photon property that can be beneficial to deep tissue or in vivo imaging. We herein designed and synthesized a new ER-targetable fluorescent probe, ER-H for imaging of ER acidification during stress in live cells and in vivo. As shown in [Scheme 1](#), ER-H contains a 1,8-naphthalimide as a highly sensitive fluorescent group, a piperazine moiety as a pH-responsive unit, a 4-methyl benzenesulphonamide moiety for ER anchoring, and a thiol reactive benzyl chloride subunit for further fixation at the ER. Under neutral pH the fluorescence of ER-H is quenched by photoinduced electron transfer (PET). Conversely, at acidic pH, through protonation-induced inhibition of PET, ER-H provides a turn-on fluorescence response. The 4-methyl benzenesulphonamide moiety endowed ER-H excellent ER targeting ability by combining with the sulfanilamide receptor in ER. Experiments demonstrated that ER-H is highly sensitive and selective to pH, and possesses high photostability and low cytotoxicity. Confocal fluorescence imaging results demonstrate that ER-H can precisely target ER and trace the acidification of ER during stress. Furthermore, due to the ideal two-photon character of 1,8-naphthalimide, by virtue of two-photon fluorescence microscope, ER-H was successfully applied for fluorescence imaging of the acidification in zebrafish and mice model.

2. Experimental

2.1. Reagents and instruments

All the reagents (purity over 99.9%) were purchased from commercial source (Sigma Aldrich, China) and used without further purification unless specified. The solvents were purified by conventional methods before use. Calcium ion sensor Fluo-3 AM, ER-Tracker Red, Mito-Tracker Green, Lyso-Tracker Deep Red, and Golgi-Tracker Red were purchased from Invitrogen (USA). 3-(4, 5-dimethylthiazol-2-yl) 2, 5-diphenyl tetrazolium bromide (MTT), tunicamycin (Tm), thapsigargin (Tg) were purchased from Sigma. Silica gel (200–300 mesh) used for flash column chromatography was purchased from Qingdao Haiyang Chemical Co., Ltd. ^1H NMR and ^{13}C NMR spectra were determined by 400 MHz and 100 MHz using Bruker NMR spectrometers. The mass spectra were obtained by Bruker maxis ultra-high resolution-TOF MS system. The fluorescence spectra measurements were performed using Hitachi F-4600 or FLS-980 Edinburgh fluorescence spectrometer. UV–vis absorption spectra were made with a TU-1900. All pH measurements were carried out on pHS-3C pH meter. The zebrafish were purchased from Eze-Rinka Company (Nanjing, China). The adult

KM mice (female, 6–8 week-old, 20 ± 2 g) were purchased from the laboratory animal center of Shandong University (Jinan, China). All animal experiments were conducted at the laboratory of Shandong Normal University in compliance with the Guidelines of Shandong Normal University for the Care and Use of Laboratory Animals. Confocal fluorescence imaging in cells, zebrafish or mice were performed with Leica TCS SP8 (one-photon) or Zeiss LSM 880 NLO (two-photon) Confocal Laser Scanning Microscope. The laser power of confocal imaging is 5.0 mW for 405, and 15 mW for 488 nm, 561 nm and 633 nm laser. The two-photon excitation wavelength is 800 nm. The hepatoma carcinoma cell (HepG2) was purchased from Cell Bank of the Chinese Academy of Sciences (Shanghai, China).

2.2. Synthesis of probe ER-H

Synthesis of compound ER-NapPZ. Under argon atmosphere, compound ER-NapBr (474 mg, 1.0 mmol), piperazine (860 mg, 10 mmol) and triethylamine (0.50 mL) were successively added to the stirred solution of 2-methoxyethanol (15 mL) in a round-bottomed flask. After heating at 100 °C for 12 h, the mixture was cooled to room temperature and poured into diethyl ether. The resulting precipitate was filtered and purified by silica gel chromatography with $\text{CH}_2\text{Cl}_2:\text{CH}_3\text{OH}$ (v/v, 5:1) as the eluent to yield ER-NapPZ as a yellow solid (250 mg, 52%). ^1H NMR (400 MHz, *d6*-DMSO) δ (ppm): 1.876 (s, 1H), 2.249 (s, 3H), 3.013–3.061 (m, 4H), 3.604 (s, 8H), 7.232 (d, $J = 8.0$ Hz, 3H), 7.598 (d, $J = 8.0$ Hz, 2H), 7.724 (t, $J = 8.0$ Hz, 2H), 8.272 (d, $J = 8.0$ Hz, 1H), 8.338–8.373 (m, 2H). ^{13}C NMR (100 MHz, *d6*-DMSO) δ (ppm): 21.34, 45.96, 54.32, 115.22, 115.75, 122.95, 125.64, 126.20, 126.83, 129.63, 129.93, 130.91, 132.56, 138.04, 142.91, 156.57, 163.46, 164.03. MS m/z calcd. for $\text{C}_{25}\text{H}_{26}\text{N}_4\text{O}_4\text{S}$ [$\text{M} + \text{H}^+$]: 479.1747, found 479.1706.

Synthesis of ER-H. Under argon atmosphere, ER-NapPZ (240 mg, 0.5 mmol), dichloro-*p*-xylene (875 g, 5.0 mmol), and K_2CO_3 (695 g, 5.0 mmol) were dissolved in CH_3CN (20 mL). The reaction mixture was then stirred and heated at reflux for 15 h before being allowed to cool to room temperature. The white precipitates (excess dichloro-*p*-xylene and KCl) were filtered off and the yellow colored filtrate was reduced in volume on the rotary evaporator. It was then purified over silica gel using $\text{CH}_2\text{Cl}_2:\text{CH}_3\text{OH}$ (v/v, 10:1) as the eluent. This gave ER-H as a yellow solid (123 mg, 40%). ^1H NMR (400 MHz, *d6*-DMSO) δ (ppm): 2.259 (s, 3H), 2.706 (s, 4H), 3.063 (q, $J = 6.0$ Hz, 2H), 3.2423 (s, 4H), 3.634 (s, 2H), 4.084 (t, $J = 6.0$ Hz, 2H), 4.771 (s, 2H), 7.240 (d, $J = 8.0$ Hz, 2H), 7.308 (d, $J = 8.0$ Hz, 1H), 7.376–7.442 (m, 3H), 7.598 (d, $J = 8.0$ Hz, 2H), 7.728–7.792 (m, 2H), 8.331 (d, $J = 8.0$ Hz, 1H), 8.411 (d, $J = 7.2$ Hz, 2H). ^{13}C NMR (100 MHz, *d6*-DMSO) δ (ppm): 21.35, 46.52, 53.00, 53.37, 62.01, 62.23, 115.42, 116.09, 123.07, 125.69, 126.41, 126.82, 129.30, 129.65, 129.72, 129.94, 130.88, 131.00, 132.54, 136.90, 138.05, 138.74, 142.92, 156.01, 163.52, 164.08. MS m/z calcd. for $\text{C}_{33}\text{H}_{33}\text{ClN}_4\text{O}_4\text{S}$ [$\text{M} + \text{H}^+$]: 617.1984, found 617.1984.

2.3. Preparation of other active species

In all the in vitro experiments, the metal ions were presented in the chloride. H_2O_2 was diluted appropriately in double-distilled water. The concentration of H_2O_2 was determined based on the molar extinction coefficient at 240 nm ($43.6 \text{ M}^{-1} \text{ cm}^{-1}$). NaOCl solution was diluted appropriately in 0.1 M NaOH aq. The concentration of OCl^- was determined based on the molar extinction coefficient at 292 nm ($350 \text{ M}^{-1} \text{ cm}^{-1}$). Glutathione (GSH), cysteine (Cys), and homocysteine (HCys) were dissolved in double-distilled water.

2.4. Procedure for fluorescence measurement

ER-H was dissolved in dimethyl sulfoxide (DMSO) to produce a stock solution (1.0 mM). The solutions were diluted in PBS buffer

(20 mM, containing 10% DMSO) with different pH values to the lowest concentration of 10 μ M. For the selectivity experiment, relevant active molecules were prepared as stock solution in water. Appropriate amounts of biologically relevant analytes were added to separate portions of the solution and mixed thoroughly with 10 μ M ER-H at pH 7.4. Hitachi F-4600 fluorescence spectrometer was used to acquire the fluorescence spectra. The slit width was set to 5.0 nm. For the fluorescence photostability and kinetic assays, fluorescence intensity at 528 nm was collected in FLS-980 fluorescence spectrophotometer immediately upon ER-H was added to different pH values.

2.5. Cells culture and imaging

HepG2 cells were cultured in Dulbecco's modified Eagle's medium (DMEM, Invitrogen) supplemented with 10% fetal bovine serum (Invitrogen), 1.0% penicillin and 1.0% streptomycin. The cells were seeded in confocal culture dishes and then incubated for 24 h at 37 °C under a humidified atmosphere containing 5.0% CO₂. For colocalization cell imaging experiments, the cells were seeded onto glass plates for 24 h for adherence, then washed by PBS and incubated with the probe ER-H or corresponding commercial dyes before fluorescence imaging. For ER stress experiments, the HepG2 cells were incubated with ER-H (or with Fluo-3 AM) for 30 min, then washed with PBS for three times, and Tm or Tg was added. The fluorescence images were collected at different times. To test the cytotoxicity of ER-H, the cell viability of HepG2 cells was determined by MTT assay. Fluorescence imaging in cells with ER-H were performed on Leica TCS SP8 one-photon Confocal Laser Scanning microscope.

2.6. Zebrafish and live mice imaging

Zebrafish were incubated with ER-H (20 μ M) at different pH values for 40 min. Then the zebrafish were washed with PBS (pH 7.4) for three times. And the fluorescence images were captured with Zeiss LSM 880 NLO Confocal Laser Scanning Microscope by a 800 nm two-photon laser. For time-dependent fluorescence imaging, zebrafish were incubated with ER-H (20 μ M). Then the zebrafish were acidified with buffer (pH 4.0), then the two-photon fluorescence images were acquired at different time. For live mice imaging, the mice were intraperitoneally injected with different pH buffer after anesthetization, and ER-H (100 μ M) was injected subsequently. Then the abdominal tissues were imaged with a 800 nm two-photon laser. For time-dependent fluorescence imaging, mice tissues were incubated with ER-H (100 μ M). Then the abdominal tissues were acidified with buffer (pH 4.0), and the two-photon fluorescence images were acquire at different time. For visualization of the intrinsic acidification, mice were treated with PBS or tunicamycin for 6 h, then the two-photon fluorescence images were acquired.

3. Results and discussion

3.1. Synthesis of the probe ER-H

As shown in Scheme 2, ER-H was easily synthesized by two steps. ER-NapBr has been synthesized and reported by our previous work [43,44]. Reaction of compound ER-NapBr and piperazine produced ER-NapPZ. Subsequently, ER-H was obtained from ER-NapPZ with dichloro-*p*-xylene in CH₃CN. The final structures of ER-NapPZ and ER-H were well characterized with ¹H NMR, ¹³C NMR and HRMS.

3.2. The spectroscopic response of ER-H to pH

We first test whether ER-H can respond to different pH values. As shown in Fig. 1A, at acidic condition (pH < 4.0), the probe ER-H displayed an absorption maximum centered at about 395 nm. However, when the pH increase from 3.0 to 9.0, the absorption maximum shifted

to about 415 nm, exhibiting almost no changes in the absorption intensity. Meanwhile, the fluorescence spectra of probe ER-H at different pH values were detected (Fig. 1B). Upon excited at 400 nm, the probe displayed almost no fluorescence at neutral and alkaline pH. Along with the pH varied from 9.5 to 2.5, an emission peak evolved at 528 nm and the fluorescence intensity increased gradually (Fig. 1C). This result indicated that the acidic pH indeed inhibited the PET in ER-H and recovered the fluorescence of 1,8-naphthalimide, suggesting that ER-H has a turn-on fluorescence response to acidic pH. More data displayed that the fluorescence emission intensity at 528 nm showed a good linear relationship with the pH values ranging from 4.0 to 5.0 (Fig. 1D). And the pK_a of the probe was calculated to be 4.58 (Fig. S1), which further illustrated that the probe was a sensitive acid-responsive sensor. Considering that ER stress will cause ER autophagy, the pH of ER will decrease to acidic condition. The results manifested that probe ER-H was expected to be suitable for imaging the acidification of ER.

3.3. Selectivity of ER-H to pH

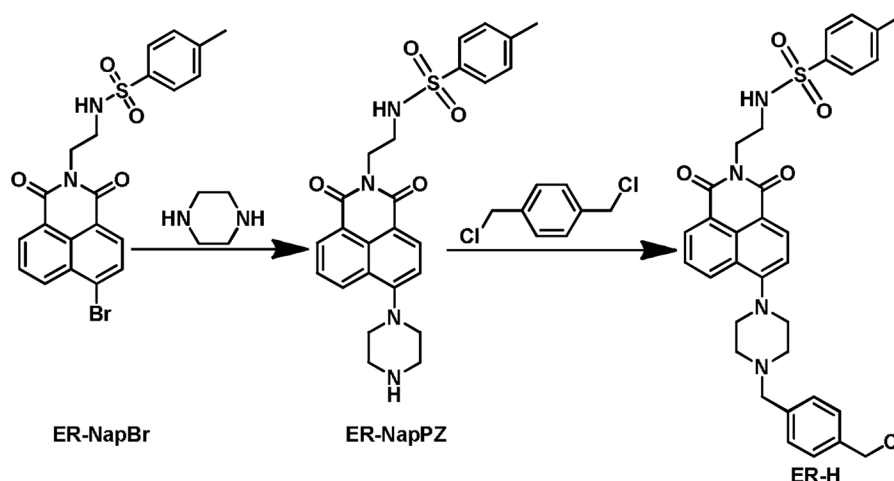
Next, in order to examine whether ER-H can specifically respond to pH, we detected the fluorescence spectra of ER-H in the presence of various bioactive molecules, including common metal ions, reactive oxygen species (ROS), thiols. Under physiological condition (pH 7.4), ER-H alone displayed weak fluorescence, and after addition of above-mentioned analytes, the fluorescence spectra of ER-H showed almost no changes compared to that of ER-H alone. In sharp contrast, the fluorescence of ER-H exhibited significant enhancement under acidic condition at pH 4.0 (Fig. 2A and B). In addition, MTT assay demonstrated that ER-H was almost non-cytotoxic (Fig. S2). Therefore, all these data demonstrated that ER-H displayed excellent selectivity for pH over other species had favorable biocompatibility, which may be applied for detection of acidification in complex biological system.

3.4. Photostability and kinetic studies

We next tested the photostability of ER-H at different pH values. The fluorescence intensity of ER-H for 528 nm at pH 7.0 and 3.0 was recorded continuously under 400 nm laser. As shown in Fig. S3A, ER-H exhibited obvious higher fluorescence intensity at 528 nm under pH 3.0, and the fluorescence intensity of ER-H was almost changeless under continuous 600 s irradiation. To further confirm the pH dependence of ER-H, real-time fluorescence variations of ER-H in different pH environments were recorded. As shown in Fig. S3B, the fluorescence intensity of ER-H increased immediately in an acidic buffer solution after addition of HCl solution. However, when the acidic solution was adjusted to neutral or alkaline conditions by addition of NaOH solution, the fluorescence intensity instantly decreased. Again, after the solution was adjusted back to acidic conditions, the fluorescence emission continued to increase at once. All these experiments demonstrated that ER-H was photostable and can real-time respond to acidic pH values.

3.5. Cell imaging experiments

With this excellent probe in hand, we next intended to test the application of ER-H in live cells fluorescence imaging. We first tested the ER targetable ability of ER-H. HepG2 cells were incubated with ER-H and ER-Tracker Red, a commercial ER dye for 30 min. After washed with PBS for three times, the HepG2 cells were imaged with confocal fluorescence microscope. As shown in Fig. 3B, ER-H displayed distinguishable fluorescence in green channel. Meanwhile, the colocalization experiment results within these HepG2 cells suggested that the green fluorescence of ER-H overlapped well with the red fluorescence of ER-tracker Red (Fig. 3D), with a high colocalization coefficient of 0.90. The local magnification imaging data implied that ER-H indeed solely accumulated into ER (Fig. 3A1–D1). Further colocalization experiments implied that ER-H rarely located in mitochondria, lysosomes, and Golgi



Scheme 2. The facile synthesis of ER-H.

apparatus (Fig. S4). All the above data illustrated that ER-H is membrane-permeable and can exclusively target ER, which is prone to reporting the pH fluctuations.

When cells undergo persistent ER stress, autophagy will initiate [13]. The ER will be engulfed by lysosomes and the pH of ER will become acidic. To further explore the bioapplication of ER-H, we want to utilize ER-H to visualize the acidification of ER during stress in real-time. After incubated with ER-H (10 μM) for 30 min, HepG2 cells were stimulated with tunicamycin (Tm, 10 $\mu\text{g}/\text{mL}$) that is an inhibitor of protein N-glycosylation and can a trigger ER stress [45]. The time-

dependent fluorescence images of HepG2 cells were exhibited in Fig. 4A. It showed that the fluorescence intensity of ER-H risen obviously (Fig. 4B), indicating the acidification of ER under autophagy. Additionally, when cells were stimulated with thapsigargin (Tg, 1.0 $\mu\text{g}/\text{mL}$), an inhibitor of the ubiquitous ER Ca^{2+} -ATPases in mammalian cells, which can also cause ER stress [46], the pH of ER also decreased dramatically (Fig. 4C and D). In contrast, the fluorescence of ER-H showed no increase without ER stress, suggesting the pH of ER didn't change under this condition (Fig. S5). Further, we performed the colocalization experiment between ER and lysosome in the condition of

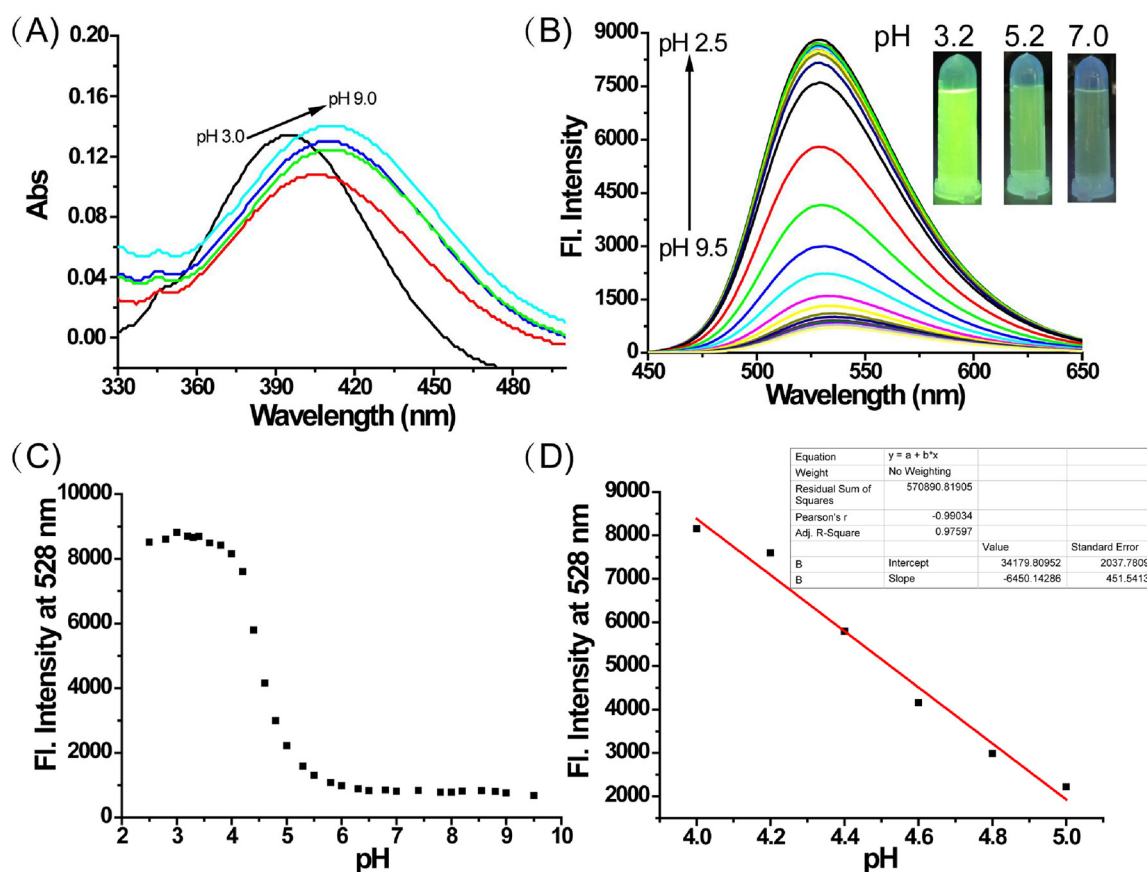


Fig. 1. (A) The absorption spectra of ER-H (10 μM) at different pH values. (B) The fluorescence spectra of ER-H (10 μM) at different pH values. Inset: Fluorescence images of ER-H under a 365 nm laser. (C) The relationship of fluorescence intensity at 528 nm and different pH values. (D) The relationship of fluorescence intensity at 528 nm and pH values ranging from 4.0 to 5.0. Ex = 400 nm.

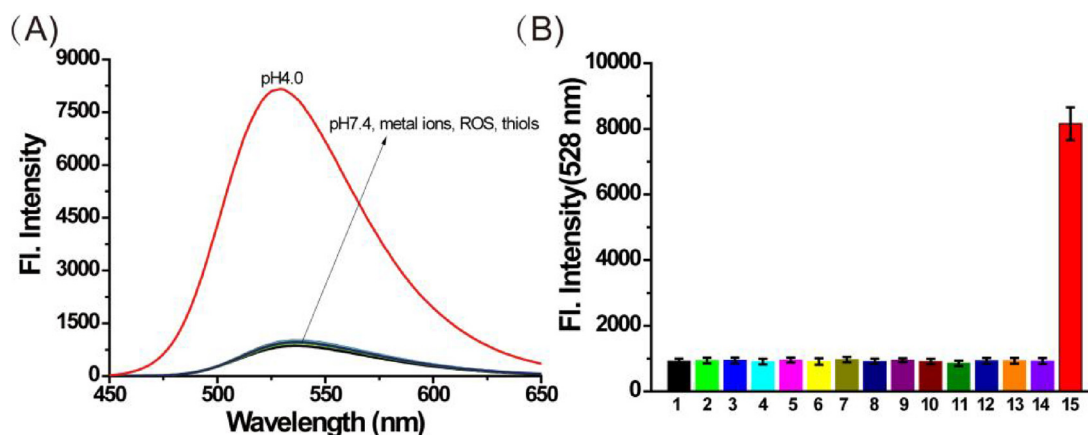


Fig. 2. (A) The fluorescence spectra of ER-H (10 μ M) with various analytes at pH 7.4 and the fluorescence spectrum of ER-H at pH 4.0. (B) The fluorescence intensity of ER-H at 528 nm after addition of various analytes. 1: blank; 2: Na^+ , 10 mM; 3: K^+ , 10 mM; 4: Ca^{2+} , 500 μ M; 5: Mg^{2+} , 500 μ M; 6: Zn^{2+} , 500 μ M; 7: Al^{3+} , 100 μ M; 8: Cu^{2+} , 100 μ M; 9: Fe^{3+} , 100 μ M; 10: GSH, 5.0 mM; 11: Cys, 5.0 mM; 12: HCys, 5.0 mM; 13: H_2O_2 , 10 mM; 14: NaClO, 100 μ M; 15: pH 4.0. Ex = 400 nm. Fluorescence profiles were obtained with a Hitachi F-4600 fluorometer, and the slits were 3.0 and 3.0 nm.

ER stress. As shown in Fig. S6, under normal physiological condition, the fluorescence of ER-H and Lyso-Tracker Deep Red (the commercial lysosomes dye) displayed almost no overlay, however, in the Tg-treated cells, they exhibited some correlation. The data manifest that during ER stress, autophagy can occur and contribute to the acidification of ER. The level fluctuations of pH under such conditions can be monitored by ER-H, which confirmed that ER-H is capable of real-time imaging ER acidification in living cells.

It was reported that Tg could block Ca^{2+} -ATPase in the ER and thus depletes ER calcium ion and elevate the cytoplasmic calcium ion [47]. To further visualize the synergetic variation of ER pH and cytoplasmic calcium ion, we utilized ER-H and a calcium ion sensor Fluo-3 AM [48] for simultaneous imaging during Tg-induced ER stress. After incubated with ER-H and Fluo-3 AM for 30 min, HepG2 cells were stimulated with Tg. The real-time fluorescence imaging results were displayed in Fig. 5A. As expected, during treated with Tg, HepG2 cells stained with ER-H and Fluo-3 AM displayed a successive increment of the fluorescence intensity, indicating the decrease of ER pH and rise of

cytoplasmic calcium ion. All these data confirmed that ER-H combining with Fluo-3 AM can realize the simultaneous fluorescence imaging of ER acidification and calcium ion release from ER during stress.

3.6. Zebrafish and mice imaging experiments

Having established the ability of ER-H to detect ER acidification in live cells, we next investigated its capability to determinate pH difference in vivo. Considering the fluorophore 1,8-naphthalimide in ER-H is an ideal two-photon dye [49,50], we firstly took advantage of two-photon microscope for imaging different pH values in zebrafish. For this purpose, the zebrafish were incubated with different pH buffer solution containing 20 μ M ER-H for 40 min. After removed the solution, the two-photon fluorescence imaging of zebrafish were carried out by using two-photon fluorescence microscope with a 800 nm laser. As shown in Fig. 6, ER-H exhibited weak fluorescence in neutral condition at pH 7.0. In sharp contrast, with the decrease of pH from 7.0 to 3.0, ER-H displayed enhance fluorescence. Moreover, the time-course two-photon

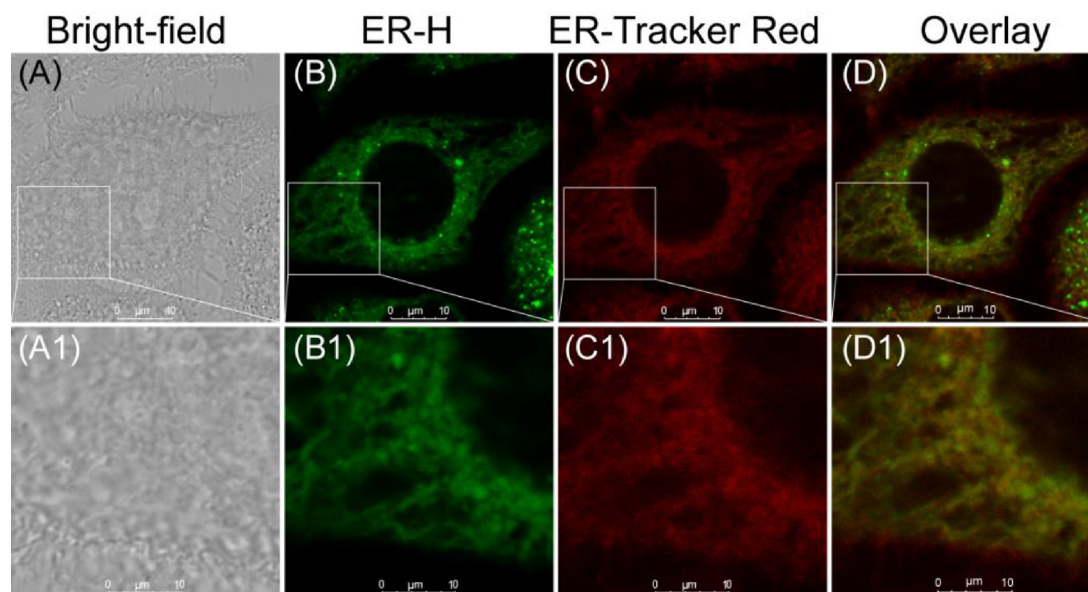


Fig. 3. Confocal fluorescence imaging of HepG2 cells stained with ER-H and ER-Tracker Red. (A) The bright-field image. (B) The fluorescence image from ER-H (10 μ M, Ex = 405 nm, collected 500–550 nm). (C) The fluorescence image from ER-Tracker Red (500 nM, Ex = 561 nm, collected 600–650 nm). (D) The overlay image between B and C. (A1–D1) The magnification images from the white boxes in A–D. Scale bar: 10 μ m. (For interpretation of the references to colour in this figure legend, the reader is referred to the web version of this article).

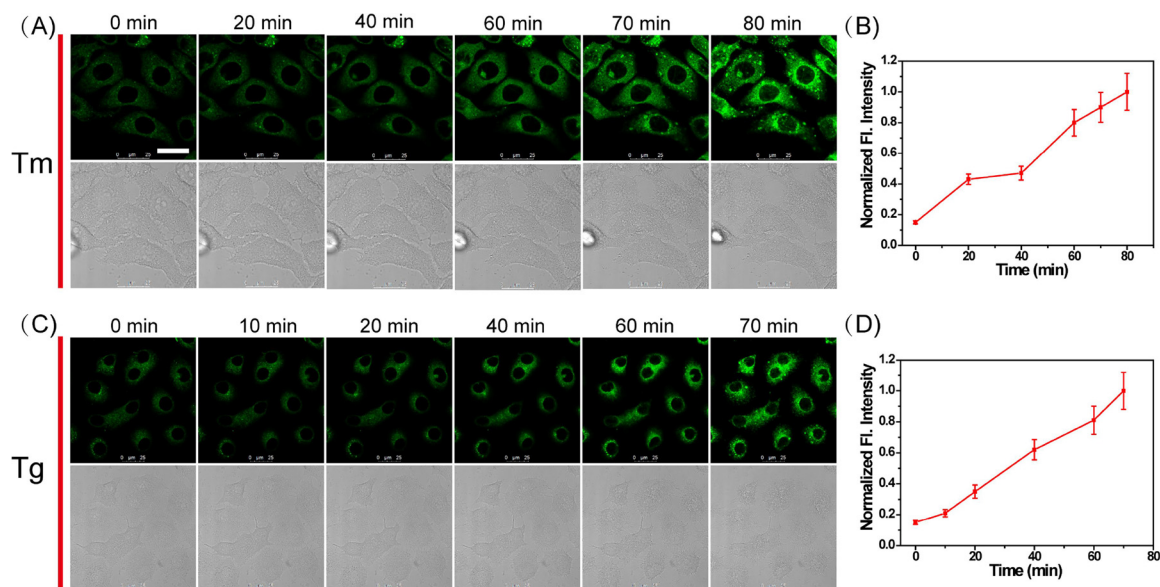


Fig. 4. The time-dependent fluorescence imaging of HepG2 cells incubated with ER-H during ER stress. (A) The fluorescence images of HepG2 cells incubated with ER-H ($10\ \mu\text{M}$) for 30 min then treated with $10\ \mu\text{g}/\text{mL}$ Tm. (B) The output of normalized average fluorescence intensity from A. (C) The fluorescence images of HepG2 cells incubated with ER-H ($10\ \mu\text{M}$) for 30 min then treated with $1.0\ \mu\text{g}/\text{mL}$ Tg. (D) The output of normalized average fluorescence intensity from C. Ex = 405 nm, Em = 500–550 nm. Scale bar: $25\ \mu\text{m}$.

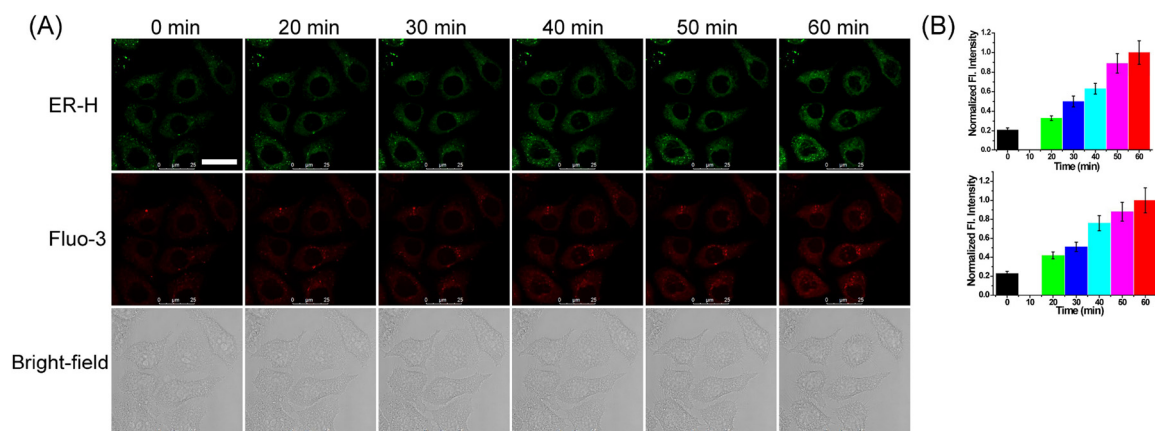


Fig. 5. The time-dependent fluorescence imaging of HepG2 cells incubated with ER-H and Fluo-3 AM during Tg-induced ER stress. (A) The fluorescence images of HepG2 cells incubated with ER-H ($10\ \mu\text{M}$) and Fluo-3 AM ($100\ \text{nM}$) for 30 min then treated with $1.0\ \mu\text{M}$ Tg. Green channel: images for ER-H, Ex = 405 nm, Em = 500–550 nm. Red channel: images for Fluo-3 AM, Ex = 488 nm, Em = 500–550 nm. Scale bar: $25\ \mu\text{m}$. (B) The output of normalized average fluorescence intensity from A. (For interpretation of the references to colour in this figure legend, the reader is referred to the web version of this article).

fluorescence imaging of zebrafish verified the pH-dependence and availability of ER-H (Fig. S7). This result suggested that ER-H can be used to two-photon fluorescence imaging and can distinguish the pH difference in zebrafish.

We subsequently explored the application of ER-H for visualization of pH difference in mice. For this purpose, the left and right sides of the abdomen of Kunming mice were incubated with different buffer solutions at pH 7.4 and pH 4.0, respectively. Next, ER-H ($100\ \mu\text{M}$, $100\ \mu\text{L}$) was injected into the abdomen (Fig. 7A). Confocal fluorescence imaging was performed immediately. As shown in Fig. 7B, ER-H within pH 7.4 emitted weak fluorescence in different depths of the left abdomen. On the contrary, after acidification in the right abdomen, ER-H displayed intense fluorescence. The 3D stack images further verified the obvious higher fluorescence of ER-H in the acidic condition. Similarly, the time-course two-photon fluorescence imaging of mice tissue indicated the excellent availability of ER-H (Fig. S8). Additionally, two-photon fluorescence images of pH difference in normal or Tm-stimulated abdominal tissues indicated that ER-H can monitor the intrinsic acidification of ER under stress (Fig. S9). All these data demonstrate that

ER-H is an ideal sensor for visualization of the pH difference in abdomen tissues of mice.

4. Conclusions

In conclusion, we have designed and synthesized a new ER-targetable pH-responsive fluorescent probe ER-H for real-time imaging of ER acidification in live cells and in vivo. ER-H can respond to acidic pH condition by protonation-induced inhibition of PET. ER-H is able to distinguish pH from other interferents with high selectivity, rapid response, excellent sensitivity. The probe ER-H could exclusively aggregate into ER and visualize the acidification process in HepG2 cells during ER stress. Moreover, the decrease of ER pH value and increase of cytoplasmic calcium ion was also imaged by simultaneous fluorescence imaging with ER-H and Fluo-3 AM. Additionally, by utilizing two-photon fluorescence microscope, we imaged the pH difference with ER-H in zebrafish and abdominal tissues of live mice. We expect that ER-H might be developed to a good pH-sensitive fluorescent probe for real-time visualization of ER acidification, which will help to elucidate the

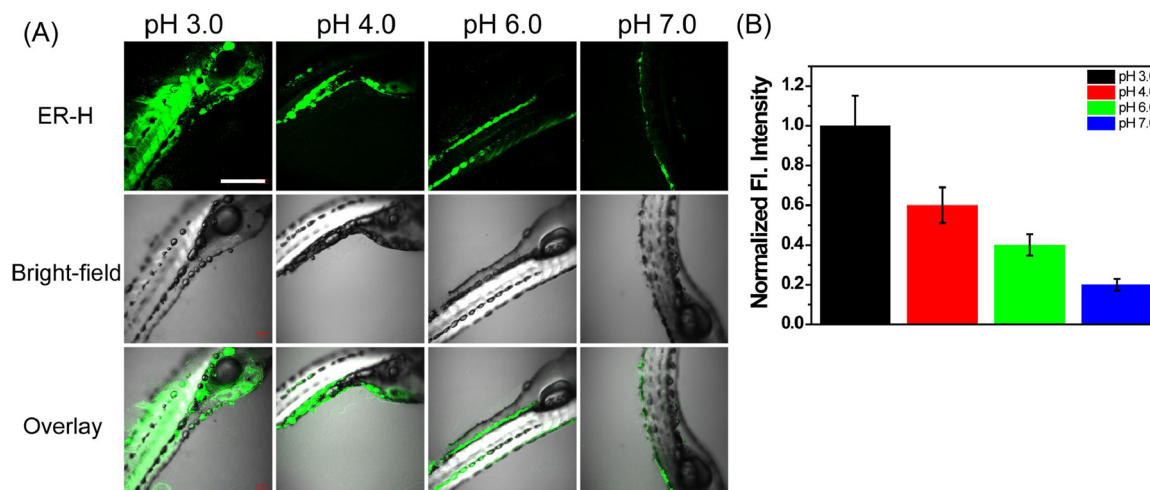


Fig. 6. Two-photon fluorescence imaging of pH difference in zebrafish incubated with ER-H. (A) The fluorescence images of zebrafish incubated with ER-H (20 μ M) for 40 min at different pH buffer solutions. Ex = 800 nm, Em = 500–550 nm. (B) The output of normalized average fluorescence intensity from A. The fluorescence intensity statistics was output by selecting five representative regions. Scale bar: 400 μ m.

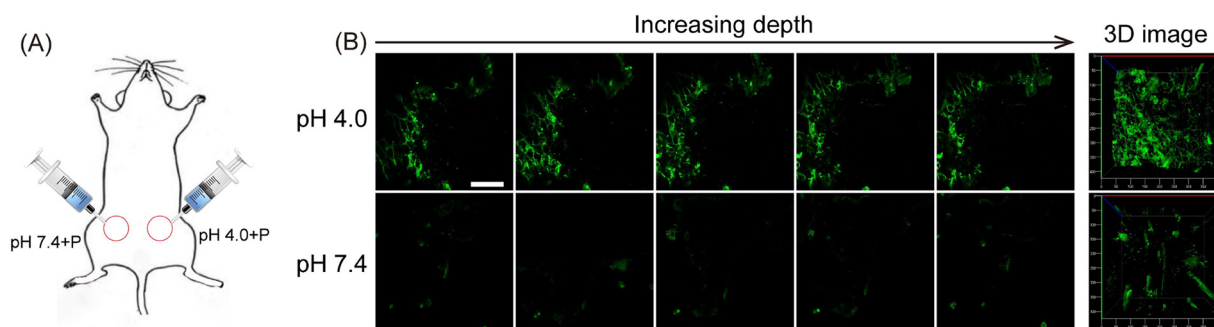


Fig. 7. Two-photon fluorescence imaging of pH difference in abdominal tissues of mice. (A) The schematic image of the treated mice. (B) Left: The selected fluorescence images of abdominal tissues incubated with ER-H (100 μ M) at PBS (pH 7.4 or pH 4.0). Right: The 3D stack images. Ex = 800 nm, Em = 500–600 nm. Scale bar: 400 μ m.

vital role of pH changes in occurrence and development of ER stress associated diseases.

Acknowledgements

This work was supported by the National Natural Science Foundation of China (21535004, 91753111, 21390411, 21675105, 21475079), National Major Scientific and Technological Special Project for “Significant New Drugs Development” (2017ZX09301030004) and the Natural Science Foundation of Shandong Province of China (ZR2017ZC0225).

Appendix A. Supplementary data

Supplementary material related to this article can be found, in the online version, at doi:<https://doi.org/10.1016/j.snb.2018.07.059>.

References

- [1] A. Görlach, P. Klappa, T. Kietzmann, The endoplasmic reticulum: folding, calcium homeostasis, signaling, and redox control, *Antioxid. Redox Signal.* 8 (2006) 1391–1418.
- [2] R. Sitia, I. Braakman, Quality control in the endoplasmic reticulum protein factory, *Nature* 426 (2003) 891–894.
- [3] L. Ellgaard, A. Helenius, Quality control in the endoplasmic reticulum, *Nat. Rev. Mol. Cell Biol.* 4 (2003) 181–191.
- [4] C. Xu, B. Bailly-Maitre, J.C. Reed, Endoplasmic reticulum stress: cell life and death decisions, *J. Clin. Invest.* 115 (2005) 2656–2664.
- [5] K. Zhang, R.J. Kaufman, From endoplasmic-reticulum stress to the inflammatory response, *Nature* 454 (2008) 455–462.
- [6] R.V. Rao, D.E. Bredesen, Misfolded proteins, endoplasmic reticulum stress and neurodegeneration, *Curr. Opin. Cell Biol.* 16 (2004) 653–662.
- [7] U. O’zcan, Q. Cao, E. Yilmaz, A.H. Lee, N.N. Iwakoshi, E. O’zden, G. Tuncman, C. Görgün, L.H. Glimcher, G.S. Hotamisligil, Endoplasmic reticulum stress links obesity, insulin action, and type 2 diabetes, *Science* 306 (2004) 457–461.
- [8] D.L. Eizirik, A.K. Cardozo, M. Cnop, The role for endoplasmic reticulum stress in diabetes mellitus, *Endocr. Rev.* 29 (2007) 42–61.
- [9] W.H. Moolenaar, Effects of growth factors on intracellular pH regulation, *Annu. Rev. Physiol.* 48 (1986) 363–376.
- [10] D. Lagadic-Gossmann, L. Huc, V. Lecœur, Alterations of intracellular pH homeostasis in apoptosis: origins and roles, *Cell Death Differ.* 11 (2004) 953–961.
- [11] F.A. Smith, J.A. Raven, Intracellular pH and its regulation, *Ann. Rev. Plant Physiol.* 30 (1979) 289–311.
- [12] J.H. Kim, L. Johannes, B. Goud, C. Antony, C.A. Lingwood, R. Daneman, S. Grinstein, Noninvasive measurement of the pH of the endoplasmic reticulum at rest and during calcium release, *Proc. Natl. Acad. Sci. U. S. A.* 95 (1998) 2997–3002.
- [13] T. Yorimitsu, U. Nair, Z. Yang, D.J. Klionsky, Endoplasmic reticulum stress triggers autophagy, *J. Biol. Chem.* 281 (2006) 30299–30304.
- [14] D. Senft, Z.A. Ronai, UPR, autophagy, and mitochondria crosstalk underlies the ER stress response, *Trends Biochem. Sci.* 40 (2015) 141–148.
- [15] M. Høyer-Hansen, M. Jaattela, Connecting endoplasmic reticulum stress to autophagy by unfolded protein response and calcium, *Cell Death Differ.* 14 (2007) 1576–1582.
- [16] H. Yoshida, ER stress and diseases, *FEBS J.* 274 (2007) 630–658.
- [17] J.V. Frangioni, In vivo near-infrared fluorescence imaging, *Curr. Opin. Chem. Biol.* 7 (2003) 626–634.
- [18] V. Ntziachristos, C. Bremer, R. Weissleder, Fluorescence imaging with near-infrared light: new technological advances that enable in vivo molecular imaging, *Eur. Radiol.* 13 (2003) 195–208.
- [19] X. Chen, F. Wang, J.Y. Hyun, T. Wei, J. Qiang, X. Ren, I. Shin, J. Yoon, Recent progress in the development of fluorescent, luminescent and colorimetric probes for detection of reactive oxygen and nitrogen species, *Chem. Soc. Rev.* 45 (2016) 2976–3016.
- [20] M. Vendrell, D. Zhai, J.C. Er, Y.T. Chang, Combinatorial strategies in fluorescent probe development, *Chem. Rev.* 112 (2012) 4391–4420.

- [21] L. Yuan, W. Lin, K. Zheng, L. He, W. Huang, Far-red to near infrared analyte-responsive fluorescent probes based on organic fluorophore platforms for fluorescence imaging, *Chem. Soc. Rev.* 42 (2013) 622–661.
- [22] H.M. Kim, B.R. Cho, Small-molecule two-photon probes for bioimaging applications, *Chem. Rev.* 115 (2015) 5014–5055.
- [23] X. Chen, Y. Zhou, X. Peng, J. Yoon, Fluorescent and colorimetric probes for detection of thiols, *Chem. Soc. Rev.* 39 (2010) 2120–2135.
- [24] J. Du, M. Hu, J. Fan, X. Peng, Fluorescent chemodosimeters using “mild” chemical events for the detection of small anions and cations in biological and environmental media, *Chem. Soc. Rev.* 41 (2012) 4511–4535.
- [25] R. Wang, C. Yu, F. Yu, L. Chen, Molecular fluorescent probes for monitoring pH changes in living cells, *Trac-trend, Anal. Chem.* 29 (2010) 1004–1013.
- [26] S.D. Bull, M.G. Davidson, J.M.H. van den Elsen, J.S. Fossey, A.T.A. Jenkins, Y. Jiang, Y. Kubo, F. Marken, K. Sakurai, J. Zhao, T.D. James, Exploiting the reversible covalent bonding of boronic acids: recognition, sensing, and assembly, *Acc. Chem. Res.* 46 (2012) 312–326.
- [27] M.H. Lee, J.S. Kim, J.L. Sessler, Small molecule-based ratiometric fluorescence probes for cations, anions, and biomolecules, *Chem. Soc. Rev.* 44 (2015) 4185–4191.
- [28] M.H. Lee, N. Park, C. Yi, J.H. Han, J.H. Hong, K.P. Kim, D.H. Kang, J.L. Sessler, C. Kang, J.S. Kim, Mitochondria-immobilized pH-sensitive off-on fluorescent probe, *J. Am. Chem. Soc.* 136 (2014) 14136–14142.
- [29] H. Washita, S. Torii, N. Nagahora, M. Ishiyama, K. Shioji, K. Sasamoto, S. Shimizu, K. Okuma, Live cell imaging of mitochondrial autophagy with a novel fluorescent small molecule, *ACS Chem. Biol.* 12 (2017) 2546–2551.
- [30] W. Zhang, R.T.K. Kwok, Y. Chen, S. Chen, E. Zhao, C.Y.Y. Yu, J.W.Y. Lam, Q. Zheng, B.Z. Tang, Real-time monitoring of the mitophagy process by a photostable fluorescent mitochondrion-specific bioprobe with AIE characteristics, *Chem. Commun.* 51 (2015) 9022–9025.
- [31] M.Y. Wu, K. Li, Y.H. Liu, K.K. Yu, Y.M. Xie, X.D. Zhou, X.Q. Yu, Mitochondria-targeted ratiometric fluorescent probe for real time monitoring of pH in living cells, *Biomaterials* 53 (2015) 669–678.
- [32] Q. Wan, S. Chen, W. Shi, L. Li, H. Ma, Lysosomal pH rise during heat shock monitored by a lysosome-targeting near-infrared ratiometric fluorescent probe, *Angew. Chem.* 126 (2014) 11096–11100.
- [33] B. Tang, F. Yu, P. Li, L. Tong, X. Duan, T. Xie, Wang X, A near-infrared neutral pH fluorescent probe for monitoring minor pH changes: imaging in living HepG2 and HL-7702 cells, *J. Am. Chem. Soc.* 131 (2009) 3016–3023.
- [34] J.T. Hou, W.X. Ren, K. Li, J. Seo, A. Sharma, X.Q. Yu, J.S. Kim, Fluorescent bioimaging of pH: from design to applications, *Chem. Soc. Rev.* 46 (2017) 2076–2090.
- [35] T. Myochin, K. Kiyose, K. Hanaoka, H. Kojima, T. Terai, T. Nagano, Rational design of ratiometric near-infrared fluorescent pH probes with various pKa values, based on aminocyanine, *J. Am. Chem. Soc.* 133 (2011) 3401–3409.
- [36] Q. Wang, L. Zhou, L. Qiu, D. Lu, Y. Wu, X. Zhang, An efficient ratiometric fluorescent probe for tracking dynamic changes in lysosomal pH, *Analyst* 140 (2015) 5563–5569.
- [37] B. Dong, X. Song, C. Wang, X. Kong, Y. Tang, W. Lin, Dual site-controlled and lysosome-targeted intramolecular charge transfer-photoinduced electron transfer-fluorescence resonance energy transfer fluorescent probe for monitoring pH changes in living cells, *Anal. Chem.* 88 (2016) 4085–4091.
- [38] X. Liu, Y. Su, H. Tian, L. Yang, H. Zhang, X. Song, J.W. Foley, Ratiometric fluorescent probe for lysosomal pH measurement and imaging in living cells using single-wavelength excitation, *Anal. Chem.* 89 (2017) 7038–7045.
- [39] G. Li, B. Zhang, X. Song, Y. Xia, H. Yu, X. Zhang, Y. Xiao, Y. Song, Ratiometric imaging of mitochondrial pH in living cells with a colorimetric fluorescent probe based on fluorescein derivative, *Sens. Actuators B: Chem.* 253 (2017) 58–68.
- [40] Y. Li, Y. Wang, S. Yang, Y. Zhao, L. Yuan, J. Zheng, R. Yang, Hemicyanine-based high resolution ratiometric near-infrared fluorescent probe for monitoring pH changes in vivo, *Anal. Chem.* 87 (2015) 2495–2503.
- [41] Y. Yue, F. Huo, X. Li, Y. Wen, T. Yi, J. Salamanca, J.O. Escobedo, R.M. Strongin, C. Yin, pH-dependent fluorescent probe that can be tuned for cysteine or homocysteine, *Org. Lett.* 19 (2017) 82–85.
- [42] Y. Ge, P. Wei, T. Wang, X. Cao, D. Zhang, F. Li, A simple fluorescent probe for monitoring pH in cells based on new fluorophore pyrido[1,2-a]benzimidazole, *Sens. Actuators B: Chem.* 254 (2018) 314–320.
- [43] H. Xiao, P. Li, X. Hu, X. Shi, W. Zhang, B. Tang, Simultaneous fluorescence imaging of hydrogen peroxide in mitochondria and endoplasmic reticulum during apoptosis, *Chem. Sci.* 7 (2016) 6153–6159.
- [44] H. Xiao, C. Wu, P. Li, W. Gao, W. Zhang, W. Zhang, L. Tong, B. Tang, Ratiometric photoacoustic imaging of endoplasmic reticulum polarity in injured liver tissues of diabetic mice, *Chem. Sci.* 8 (2017) 7025–7030.
- [45] T. Nakagawa, H. Zhu, N. Morishima, E. Li, J. Xu, B.A. Yankner, J. Yuan, Caspase-12 mediates endoplasmic-reticulum-specific apoptosis and cytotoxicity by amyloid- β , *Nature* 403 (2000) 98–103.
- [46] H. Yoshida, T. Matsui, A. Yamamoto, T. Okada, K. Mor, XBP1 mRNA is induced by ATF6 and spliced by IRE1 in response to ER stress to produce a highly active transcription factor, *Cell* 107 (2001) 881–891.
- [47] O. Thastrup, P.J. Cullen, B.K. Drøbak, M.R. Hanley, A.P. Dawson, Thapsigargin, a tumor promoter, discharges intracellular Ca^{2+} stores by specific inhibition of the endoplasmic reticulum Ca^{2+} -ATPase, *Proc. Natl. Acad. Sci. U. S. A.* 87 (1990) 2466–2470.
- [48] J.Q. Zheng, Turning of nerve growth cones induced by localized increases in intracellular calcium ions, *Nature* 403 (2000) 89–93.
- [49] Y. Tang, X. Kong, A. Xu, B. Dong, W. Lin, Development of a two-photon fluorescent probe for imaging of endogenous formaldehyde in living tissues, *Angew. Chem. Int. Ed.* 55 (2016) 3356–3359.
- [50] Z.R. Dai, G.B. Ge, L. Feng, J. Ning, L.H. Hu, Q. Jin, D.D. Wang, X. Lv, T.Y. Dou, J.N. Cui, L. Yang, A highly selective ratiometric two-photon fluorescent probe for human cytochrome P450 1A, *J. Am. Chem. Soc.* 137 (2015) 14488–14495.

Haibin Xiao obtained his Ph.D. degree from Shandong Normal University in 2017. He will be a lecturer in the College of Chemistry and Chemical Engineering at Shandong University of Technology. His research interests focus on the design and synthesis of new fluorescent probes and their biological applications.

Ruilin Zhang started his undergraduate study at College of Chemistry of Shandong Normal University in 2015. Now, he is a junior student majoring in applied chemistry at Shandong Normal University. He is very interested in design and synthesis of new fluorescent probes. He joined in Ping Li's lab to perform undergraduate innovation experiment project since 2016.

Chuanchen Wu obtained his B.S. and M.S. degree at Shandong Normal University in 2013 and 2016, respectively. Currently, he is a Ph.D. student under the supervision of professor Bo Tang in the College of Chemistry at Shandong Normal University. His research interests focus on the synthesis and application of new fluorescent probes in cancer diagnosis.

Ping Li received her Ph.D. degree in 2008 from Shandong Normal University. In 1998, she joined the faculty at Shandong Normal University, where she is currently a professor of College of Chemistry, Chemical Engineering and Materials Science. She is Taishan Distinguished Professor and the leader of the Changjiang Scholars and Innovative Research Team in University. Her research interests include synthesis and bioimaging application of fluorescent probes for biologically active molecules. She has published more than 40 papers.

Wen Zhang received her Ph.D. degree from Shandong Normal University in 2015. Now, she is a lecturer in College of Chemistry at Shandong Normal University. Her research interests focus on design and synthesis of novel two-photon fluorescent probes and their biological applications.

Bo Tang is now a professor of chemistry at Shandong Normal University. He received his Ph.D. degree in 1994 from Nankai University. He began his independent career as a professor of chemistry at Shandong Normal University in 1994. In 2007, he was granted the National Science Fund for Distinguished Young Scholars in China. His research interests include the development of functional molecular probes and nanomaterials for biochemical analysis, clean synthesis of chemicals, and exploring new technology for solar energy chemical transformation and storage. He has contributed more than 300 journal articles, as well as 21 invited book chapters and reviews, and obtained 39 granted patents.